ISSN 1068-3712, Russian Electrical Engineering, 2019, Vol. 90, No. 4, pp. 347–352. © Allerton Press, Inc., 2019.
Russian Text © The Author(s), 2019, published in Elektrotekhnika, 2019, No. 4, pp. 58–64.

A Protection Device against Switching Overvoltage in DC Traction Networks

D. F. Alferov[a], *, D. V. Evsin[a], and E. V. Tskhai[a]

[a] *Research and Development Institute of Applied Physics and Automation, Moscow, 115230 Russia*

**e-mail: journal-elektrotechnika@mail.ru*

Received July 17, 2017; revised September 21, 2017; accepted September 26, 2017

Abstract—A scheme of an automatic discharge device for protection against the switching overvoltage based on a controlled vacuum discharger was proposed. The discharge device is designed for shunting the reactor of the traction substation and inductance of the dc traction network during switching overloads accompanied by the power outage. Results of the experimental research and simulation of switching characteristics of such device are presented.

Keywords: dc traction networks, switching overvoltage, protective device

DOI: 10.3103/S1068371219040023

Nonlinear overvoltage suppressors (NOSs) are finding increasing application in dc traction networks. Materials based on zinc oxide (ZnO) with a nonlinear volt–ampere characteristic are used as the active element. However, in the case of overshoot suppression with high amplitudes of ensuing long-duration current, the NOS should be assembled from the large number of the parallel-series connected elements; it leads to the increase of the leakage current, complication of the structure, large dimensional envelope and, therefore, to the decrease of reliability and cost increase of NOS-based protection device. Solution of this problem is important for facilitation of the operation of the quick-operating vacuum switches in dc traction networks.

It has been proposed to use a diode discharge device (DDD) to decrease the current load on an NOS in the case of dc power outage in inductive networks [1–3]. This device shunts the circuit after outage and it contains the series-connected high-power diode discharge resistance. Under normal operating conditions, the diode is closed and connected in a nonconducting direction relative to the network voltage. In the process of disconnection, the current starts falling, while an overvoltage proportional to the current fall is observed on the inductance and the voltage on the DDD alternates in sign, which leads to the opening of the diode. Taking into account that the overloading is mainly concentrated on the inductive traction network (smoothing reactor), it was proposed to apply the special DDD, which is installed parallel to the reactor [4]. Such a device contains a series-connected high-voltage controlled resistor and high-current diode, as well as elements of the thyristor control circuit for the voltage on the reactor. The control circuit generates a command for the opening of the discharger thyristor practically at the beginning of the current fall, at the moment of changing the voltage polarity, because at this moment the voltage polarity on the reactor corresponds to the direction of the thyristor conductivity. However, operation of this device requires time for registration of the overloading and formation of the control impulse for thyristor opening. Application of the semiconductor elements decreases the emergency resistance of the device.

The application of a quick-operating protective device on the basis of the vacuum control dischargers (VCDs) is an alternative, cheaper method for solving the problem of the protection against extra voltage and current overloading [5–7]. Such a device is able to restrict the overloading with high amplitudes of the following long-duration current. The perspectives of using VCDs in a protective device are connected with its ability to operate within the wide range of the working voltages and currents without changing the switching delay time, high resistance to emergency impacts and comparatively low cost as compared with the gas-discharge and semiconductor devices [8].

The article proposes a scheme of a DDD-based automatic protection discharge device (DD) that defends against commutation overloading.

The subject of research is a DDD-based automatic protection DD that defends against impulse overloading. The device is connected parallel to inductance L_1 that includes the inductance of the traction substation reactor and dc networks (Fig. 1). Overloading activates the DD; the part of the accumulated in the L_1 energy scatters. The discharge device contains the series-con-

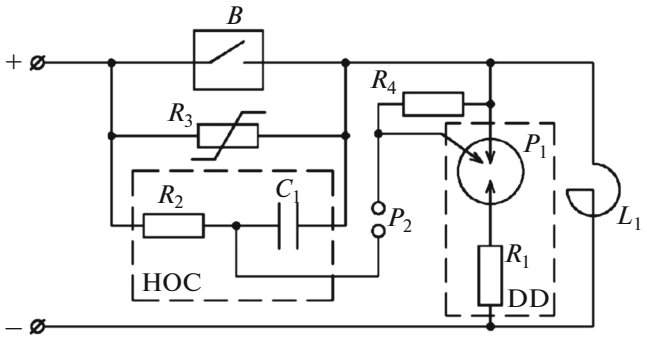

Fig. 1. Structural diagram of the discharge device.

nected discharge resistor R_1 and controlled vacuum discharger P_1 with the hands-off circuit (HOC); it contains capacitor C_1 and charging resistor R_2. The capacitor is connected by one lead to discharger P_1 and by the other lead to the control electrode of this discharger via peaking discharger P_2 with the stabilized breakdown voltage. The activation circuitry is connected parallel to nonlinear resistor R_3 (NOS) and vacuum switch B. Resistor R_4 is connected between the control electrode and cathode for the protection against the discharger false start.

The device operates in case of an overloading impulse on the inductive reactor during current outage by switch B. With an increase in voltage, capacitor C_1 starts to charge via resistor R_2 to the voltage $U_C(t)$. After breakdown voltage $U_C(t)$, discharger P_2 turns on and the voltage impulse is observed on control electrode P_1 that induces the breakthrough of the P_1 control interval initiating its start. The P_1 start moment is controlled by time constant $\tau = R_2C_1$.

The experimental scheme is given in the Fig. 2. The oscillating contour contains a capacitor battery of $C_2 =$ 50 mF for the maximum voltage of 6 kV, reactor with inductance L_1 to 6 mH and automatic quick-operating DC vacuum switch of the B type, BVV-3.3–4000/30 UXL3.

Switch B contains commutation module Q consisting of two KVD-3-2000/10 UXL2 parallel-connected vacuum arc extinguishing chambers and a counterflow contour. The commutation module of the switch is shunted by block R_3 from the four parallel-connected NOS. NOS-TP-3.0/4-YXL3 overvoltage suppressors are used as nonlinear resistors. The counterflow contour with series-connected capacitors C_3, inductance L_2, and control vacuum discharger P_4 is connected parallel to module Q.

The switch in the closed condition was connected to the preliminarily charged capacitor battery with the help of control vacuum discharger P_3; the signal for its activation was sent after charging capacitor battery C_2 to the set voltage U_0. Discharge current i started flowing in the circuit; the amplitude was regulated from the change in charge voltage U_0.

The circuit breaker opening was carried out by setting current i_{set}. The signal for switch B opening and the signal for activating discharger P_4 with a time delay of $\Delta t = 5$ ms determined by the time of the switch opening at a distance of 4 mm, were sent at $i = I_{set}$. The current with the amplitude of $I_p = U_{C3}/\sqrt{L_2/C_3} > i$ started to flow in the counter-flow circuit after activation of discharger P_4. As a result, the total current in the vacuum chamber of the commutation module fell to zero and the current was disconnected. In this case, the voltage on the switch contacts, which were suppressed by the NOS at the level of 8 kV, was quickly restored.

The investigated DD was connected in parallel to reactor L_1. The discharge device contains the control vacuum discharger P_1 and discharge resistor R_1 (Fig. 2). Discharger P_1 was activated by HOC which contains

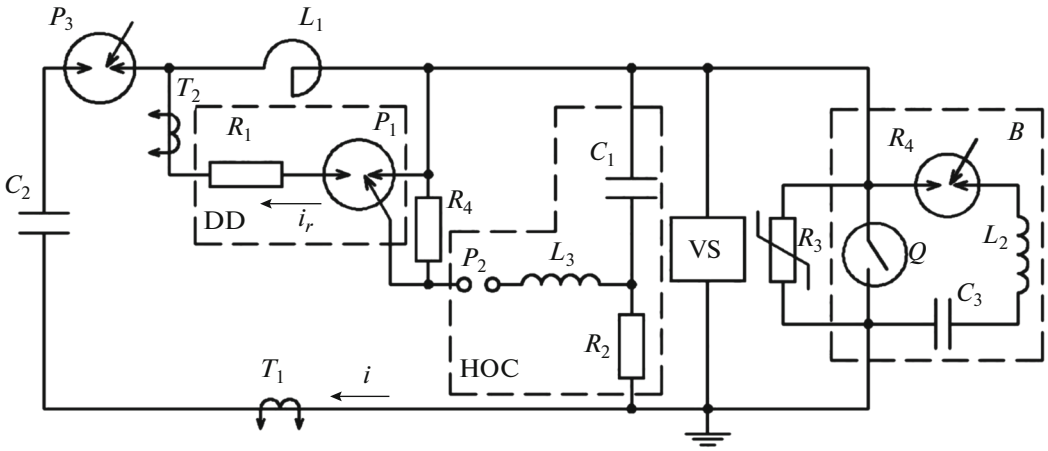

Fig. 2. Structural diagram of the test rig.

capacitor of $C_1 = 0.05$ μF, inductance is $L_3 = 11$ μH and peaking discharger P_2 with the stabilized breakdown voltage of 6 kV (Fig. 2). Capacitor C_1 charges via resistor $R_2 = 650$ Ω for 30 μs after overvoltage on resistor R_3 VCD -31N control vacuum dischargers [9] were used as dischargers P_1, P_3, and P_4.

During the tests, total current I and current i_{opn1} via the NOS (R_3) and current i_r via resistor R_1 were measured by current sensors T_1 and T_2 on the basis of the Hall effect; voltage U on the switch was measured by a voltage sensor (VS) on the basis of the Hall effect. Electrical signals were registered by a DPO-4034V digital oscillograph with the following processing of oscillograms on the personal computer.

A DD with discharge nickel–chromium resistance $R_1 = 1.8$ Ω, inductance $L_1 = 6$ mH, and current setting $I_{set} = 3$ kA was subjected to tests.

Measurement results in this mode at charge voltage of $U_0 = 3.3$ kV are given in Table 3.

After discharger P_3 was activated, current i started to flow through the switch with a rise speed of $di/dt =$ 550 A/ms; current disconnection in module Q was observed after 10.5 ms when the current reached $I_{br} = I_{set} + (di/dt)\Delta t = 5$ kA. After disconnection of the current, voltage on the switch U increased rapidly to 8 kV; activation of the DD and division of discharge current i for current i_{opn} in circuit R_3 and current i in the DD was observed near the voltage maximum. At this moment, current i_{opn} was 2 kA (about $1/3I_{br}$) and it falls quickly for 4 ms. At this time the deferred drop of voltage U on the NOS was observed. The other part of discharge current i_r flows in the DD; at the initial moment, it was 2.9 kA. Then, against background of the voltage deferred drop, the deferred i_r current drop was observed. After completion of the i_{opn} current drop, the exponential drop of current i_r, with constant time $\tau = L_1/R_1 \approx 3.3$ ms for 16 ms, started. During the current drop, the voltage on the switch smoothly decreases down to the residual voltage on the capacitor battery.

The main element determining the DD protection properties is discharge resistor R_1. Upon the set R_1 value the DD characteristics depend on the line voltage and the breaking current. In addition, they are mainly determined by the shunting inductance. Taking into account the wide range of parameters influencing on the choice of the discharge resistor, the numerical simulation of the transition processes in DD at different parameters of the electrical network was carried out.

Simulation was carried out in the MATLAB 6.5 package with the use of the Simulink 4.1 application and Sim Power Systems (SPS) library.

Figure 4 shows a structural diagram of the SPS model used for computation of the commutation process during the experiment (Fig. 2). Keys S_1, S_2, and S_3, which are responsible for commutation of dischargers P_1, P_2, and P_3 and key S_4, which simulates commutation module Q, were designed with the help of an ac switch block. The keys were broken by the current decreasing to zero. The sequences of operation of the model and experimental scheme are similar. Key S_2 closes at the zero moment of time, and control of keys S_1, S_3, and S_4 is carried out from control blocks CU_1, CU_3, and CU_4. To make the diagram simpler, Fig. 4 does not show the content of the blocks. Currents and voltages were registered by virtual current (current measurement) and voltage (voltage measurement) sensors, as well as by a Time Scope virtual oscillograph. The power block is used for setting the calculation parameters of the diagram. Calculation of the energy generated in the NOS and DD was performed by mathematical blocks from the Simulink library.

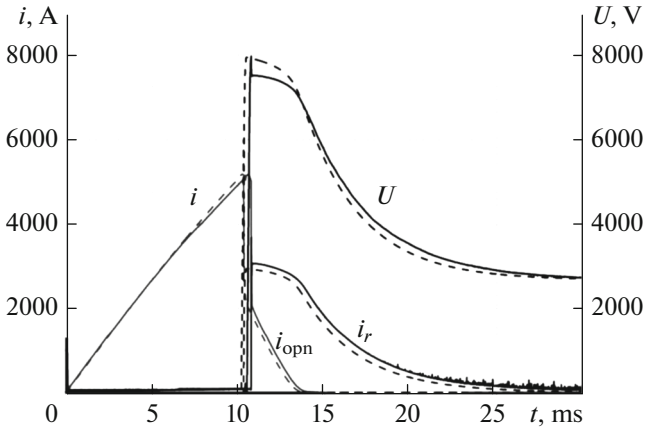

Fig. 3. Current i in discharge contour L_1C_2, current i_{opn} via resistor R_3, current i_r via the DD, and voltage U on the switch at $U_0 = 3.3$ kV. Dashed lines are results of numerical simulation.

A surge arrester was used for NOS simulation, consisting in nonlinear resistor R_3. Its volt–ampere characteristic is approximated by the combination of three exponential functions of the following type:

$$\frac{U}{U_{ref}} = k_i \left(\frac{I}{I_{ref}} \right)^{1/\alpha_i}, \qquad (1)$$

where U and I are the NOS voltage and current, U_{ref} and I_{ref} are the protective voltages, and k_i and α_i are the parameters of the ith region of the nonlinear dependence. Then, coefficients U_{ref}, I_{ref}, k_i, and α_i were determined and the model for further application was obtained by comparison of this characteristic with the actual NOS characteristic obtained from the manufacturer.

Figure 3 shows the results of modelling in the oscillating contour for charge voltage $U_0 = 3.3$ kV at reactor inductance $L_1 = 6$ mH and discharge resistor $R_1 = 1.8$ Ω by hatched lines. These results demonstrate close

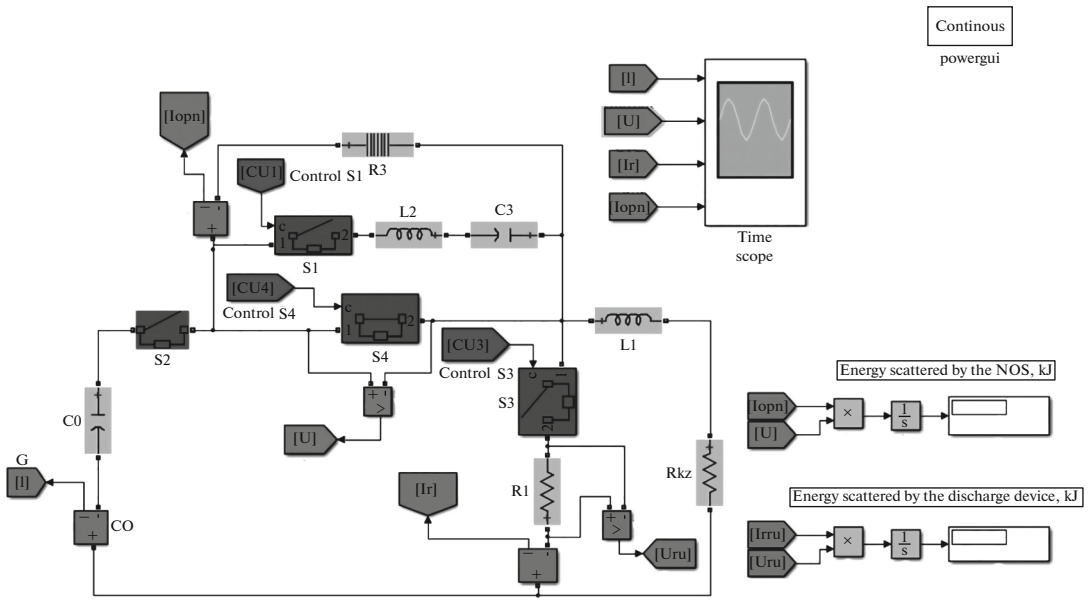

Fig. 4. Structural diagram of the SPS model.

agreement of calculation with the experiment, which demonstrates the applicability of the proposed model for selection of the DD parameters under actual conditions.

A constant-voltage source with a maximum voltage of $U_0 = 4.1$ kV with addition of active resistor $R_{sc} = 0.117$ Ω was used to study the efficiency of DD application in the traction network of Russian Railways in the structural scheme of the SPS model instead of a capacitor. With such circuit parameters, the expected maximum short-circuit current is $I_{sc} = 35$ kA. Computation results for $R_1 = 1.8$ Ω and $L_1 = 6$ mH are given in Fig. 5.

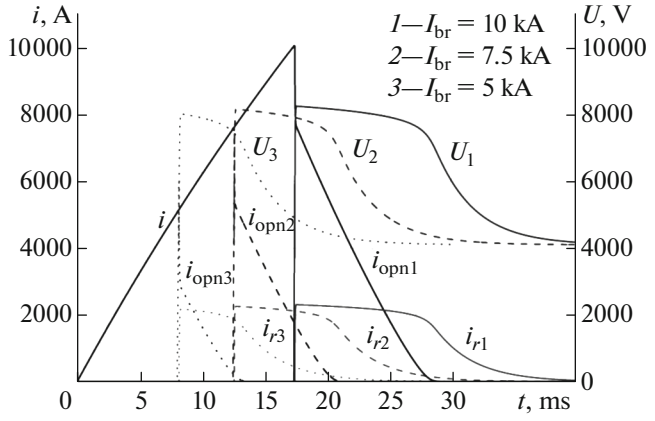

Fig. 5. Change in currents and voltages at different braking currents I_{br}: i is the current in the network before current break; i_{opn1}, i_{opn2}, and i_{opn3} are the currents via the NOS; i_{r1}, i_{r2}, and i_{r3} are the currents via the DD; and U_1, U_2, and U_3 are the voltages on a switch; I_{br} = (*1*) 10, (*2*) 7.5, and (*3*) 5 kA.

It is seen from Fig. 5 that, at a circuit break of $I_{br} = 10$ kA, the DD connects and current i splits divides into current i_{opn1} via the NOS ($i_{opn1}/I_{br} = 77\%$) and current i_{r1} via discharge resistor R_1 ($i_{r1}/I_{br} = 23\%$). With a decrease of current I_{br} to 5 kA, the share of current via the NOS i_3/I_{br} decreases to 52%.

The duration of the decrease in current in the NOS at $I_{br} = 5$ kA increased as compared with the duration of the current decrease in the oscillation contour from 3 to 5 ms (Fig. 3), possibly because of the inflow from the supply source [1]. Time t_{br} of complete current break increased as well; it consists of the current fall time in the NOS and the current fall time in discharge resistor R_1.

Figure 6 shows the dependences of time t_{br} of complete current break on the resistance of discharge resistor R_1 for different inductance L_1 at $U_0 = 4.1$ kV. As a result of simulation, it is shown that time t_{br} increases with an increase of inductance L_1 and decrease of R_1. The conditions of equality of time t_{br} of the complete current break of the BVV vacuum switch and VAB electromagnetic switch was proposed as the resistance selection criterion for the R_1 resistor. For the VAB-206 switch, time t_{br} is greatest at a network inductance of 15 mH, with a value of 50 ms [10]; this condition implies an ensuing resistance of $R_1 = 2.7$ Ω.

Energy $W_{opn} = W_L + W_0$ scatters in the DD-free network in the case of a current break in the NOS. It

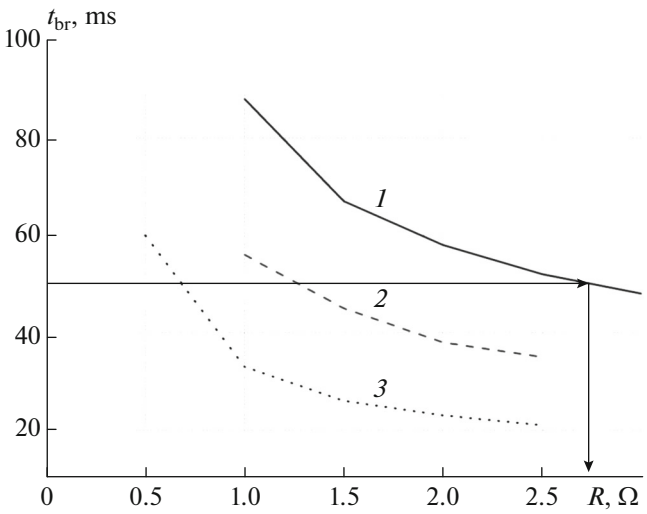

Fig. 6. Dependence of time of complete current break on resistance of the discharge resistor at L_1 = (*1*) 15, (*2*) 10, and (*3*) 5 mH.

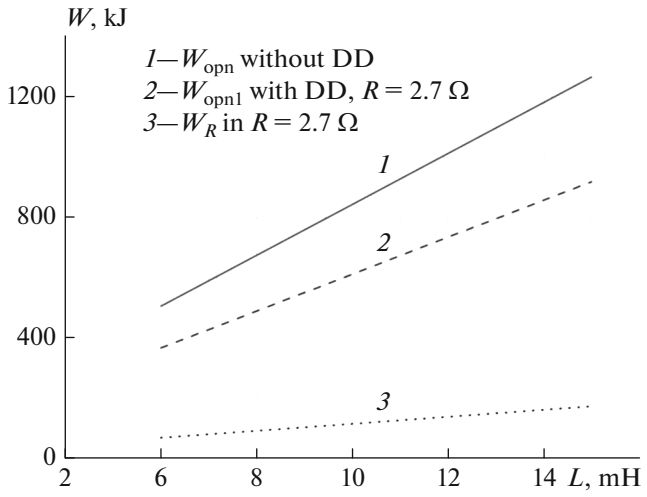

Fig. 7. Dependence of energy W scattered in an NOS and discharge resistor on inductance L_1 of the network at current break I_{br} = 10 kA and voltage U_0 = 4.1 kV: (*1*) W_{opn} in an NOS without a DD, (*2*) W_{opn1} in an NOS with a DD; energy W_R scattered in resistance of the discharge resistor R_1.

consists of energy $W_L = L_1 I_{br}^2/2$ accumulated in the network inductance and energy W_0 coming from the source. In the network with the DD, energy $W_L + W_0$ is spent on energy W_{opn1} scattered in the NOS and energy W_R scattered in discharge resistor R_1. Current i_{opn1} in the NOS with a DD and its duration are smaller than for the DD-free situation. As a consequence, the share of energy W_{opn1} coming from the source to the NOS decreases. Energy W_{opn1} depends on resistance of the discharge resistor R_1, network voltage U_0, breaking current I_{br}, and network inductance L_1. The computation dependences of energies W_{opn}, W_{opn1}, and W_R on network inductance L_1 for selected resistance R_1 = 2.7 Ω in the case of current break I_{br} = 10 kA and voltage U_0 = 4.1 kV are given in Fig. 7.

It is seen from the above results that, with a decrease in inductance, energies W_{opn} and W_{opn1} scattered in the NOS decrease proportionally:

$$\frac{W_{opn}(\text{mH}) - W_{opn1}(15\,\text{mH})}{W_{opn}(15\,\text{mH})} = \frac{W_{opn}(6\,\text{mH}) - W_{opn1}(6\,\text{mH})}{W_{opn}(6\,\text{mH})} = 27\%. \quad (2)$$

In this case, energies W_{opn1} and W_R scattered in the NOS and resistance of the discharge resistor R_1 decrease by 60% with a decrease in inductance L_1 from 15 to 6 mH.

It follows from the computation results at U_0 = 4.1 kV, L_1 = 15 mH, R_1 = 2.7 Ω, and different breaking currents that, with a decrease in the current to I_{br} = 5 kA, the share of energy W_{opn1} energy scattered in the NOS with the use of a DD decrease as follows relative to the DD-free energy scattered in an NOS:

$$\frac{W_{opn}(5\,\text{kA}) - W_{opn}(5\,\text{kA})}{W_{opn}(5\,\text{kA})} = 47\%. \quad (3)$$

Thus, the results of experiments and simulation showed that the proposed device for protecting against commutation overloading on the basis of a control vacuum discharger intended for shunting a traction substation reactor and inductance of a dc traction network contributes to decrease of energy scattered in an NOS and facilitates vacuum switch operation.

REFERENCES

1. Bei, Yu.M., Mamoshin, R.R., Pupynin, V.N., and Shalimov, M.G., *Tyagovye podstantsii* (Traction Substations), Moscow: *Transport*, 1986.
2. Pupynin, V.N. and Martyukova, V.A., Ideal DC switcher, *Elektron. Elektrooborud. Transp.*, 2013, no. 3.
3. Kalugin, I.G., Comparative efficiency of high-speed DC switchers for 13.2 kV voltage and 3 kA rated current, *ELEKTRO*, 2013, no. 6.
4. Darchiev, S.Kh. and Pupynin, V.N., RF Patent 42356, *Byull. Izobret.*, 2004, no. 33.
5. Alferov, D.F., Matveev, N.V., Sidorov, V.A., and Khabarov, D.A., Application of controlled vacuum dis-

chargers in high-voltage high-speed protective device, *Prib. Tekhn. Eksperim.*, 2004, no. 3.

6. Alferov, D.F., Evsin, D.V., Ivanov, V.P., and Sidorov, V.A., Protective device from pulsed overvoltage based on a vacuum controlled discharger, *Prib. Tekhn. Eksperim.*, 2011, no. 1.
7. Alferov, D.F., Ivanov, V.P., Miroshnichenko, V.P., Perunov, A.A., Prisenko, Yu.S., and Sidorov, V.A., Combined protective device from pulsed overvoltage, *Elektrichestvo*, 2011, no. 9.
8. Alferov, D.F., Ivanov, V.P., and Sidorov, V.A., Controlled vacuum dischargers: the main properties and application, *ELEKTRO*, 2002, no. 2.
9. Alferov, D.F., Akhmetgareev, M.R., Ivanov, V.P., and Sidorov, V.A., RF Patent 119948, *Byull. Izobret.*, 2012, no. 31.
10. TransElektroApparat company. http://www.transea.ru. Accessed June 17, 2017.

Translated by E. Grishina